Chaotic Oscillations in a Simple Collapsible-Tube Model

O. E. Jensen
Department of Applied Mathematics and Theoretical Physics, University of Cambridge, Cambridge CB3 9EW, UK;
Present address: Biomedical Engineering Department, Northwestern University, Evanston, IL 60208

A steady flow through a segment of externally pressurized, collapsible tube can become unstable to a wide variety of self-excited oscillations of the internal flow and tube walls. A simple, one-dimensional model of the conventional laboratory apparatus, which has been shown previously to predict steady flows and multiple modes of oscillation, is investigated numerically here. Large amplitude oscillations are shown to have a relaxation structure, and the nonlinear interaction between different modes is shown to give rise to quasiperiodic and apparently aperiodic behavior. These predictions are shown to compare favorably with experimental observations.

1 Introduction

When subject to negative transmural (internal minus external) pressure, an elastic-walled tube can become highly compliant, so that small pressure variations lead to large changes in the area and shape of the tube's cross-section. These area changes in turn have a profound effect on the internal flow, particularly at high Reynolds numbers when flow separation leads to the formation of a turbulent jet downstream of any severe constriction in the tube. The energy loss in such a jet lowers the internal pressure, enhancing local collapse; this is opposed by both transverse and longitudinal stresses in the tube wall. It has long been observed (e.g., [6]) that even under steady external conditions, the strong nonlinear coupling between fluid-mechanical and elastic forces can give rise to vigorous self-excited oscillations of the flow and the tube wall. These oscillations are of particular interest in the context of flows in large blood vessels because of their possible association with the Korotkoff sounds heard during sphygmomanometry [13]. They also arise spontaneously in other parts of the circulation, for example in the collapsed veins entering the thorax [12], or in the external jugular vein (which is collapsed in an upright subject), in which case they produce humming noises [7] (Prof. R. D. Kamm, personal communication).

Recent experiments by Bertram, Raymond, and Pedley [2, 3] using a rubber tube mounted between two rigid tubes and enclosed in a pressurized chamber (a "Starling Resistor," Fig. 1), have revealed a remarkable variety of such oscillations. These were classified as follows: coherent, repetitive oscillations with frequencies falling into distinct low (L), intermediate (I), and high (H) bands; noisy, more rapid oscillations with a broad-band frequency spectrum, associated in [2] with amplification of turbulent disturbances within the tube; and a number of combinations of these types, many having highly irregular waveforms. The pattern of bifurcations between different states is very rich, with abundant hysteresis and flows often highly sensitive to parameter values, as is typical of many nonlinear dynamical systems. It was suggested in [3] that some of the "irregular" oscillations may be chaotic, but unfortunately it was not possible to determine this from the available experimental data.

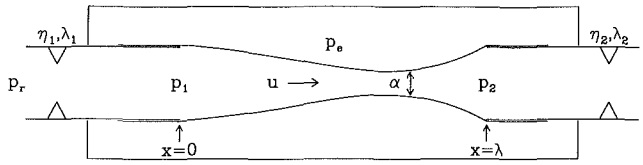

Fig. 1 The conventional laboratory apparatus: an elastic-walled tube of length λ is inserted between two rigid tubes and is enclosed in a chamber held at pressure p_e; a flow is driven from a constant head reservoir at pressure p_r and is controlled by the variable resistances η_i and inertances λ_i of upstream (i = 1) and downstream (i = 2) rigid tubes; downstream the system is open to the atmosphere. u is the longitudinal velocity within the tube and α is its cross-sectional area.

Because the Starling Resistor is important as a model of flows in both the circulation and the lung, and because of its interest as a dynamical system, a good theoretical description of its behavior is clearly desirable. The one-dimensional model of unsteady flow in a collapsed tube that is investigated here is based on that proposed by Cancelli and Pedley [5]. Its central feature is a representation of the energy losses associated with flow separation beyond a constriction in the tube. Recent analysis of the model has shown that it describes many significant experiment observations. The pressure drop-flow rate relations of its steady flows were shown in [10] to agree quantitatively with those of experiments in which thin-walled tubes were used (e.g., [4]), and qualitatively with those of Bertram [1] who, as in later experiments [2, 3], used a thicker-walled tube. A linear stability analysis in [8] showed that some of the steady flows were unstable to a family of modes of self-excited oscillation; from the ratio of their frequencies and from their distribution in parameter space, these modes could be identified with the L, I, and H oscillations observed in [2]. Weakly nonlinear theory was used to show that hysteresis can occur in the transition between steady and oscillatory states, and that doubly periodic oscillations are possible.

Fully nonlinear oscillations were obtained numerically with

Contributed by the Bioengineering Division for publication in the JOURNAL OF BIOMECHANICAL ENGINEERING. Manuscript received by the Bioengineering Division August 6, 1991; revised manuscript received September 30, 1991.

this model in [5] and [11], although it was concluded in [5] (on the basis of a limited number of calculations) that large-amplitude behavior would not arise unless the separation point was allowed to move hysteretically in response to an unsteady adverse pressure gradient. A simpler, quasi-steady condition, that is easier to implement both analytically and numerically, will be used here. Not only does this allow use of the results of [8] and [10] in guiding a study of parameter space, but it will be shown that this simplified model predicts large amplitude oscillations that share some of the relaxation structure characteristic of experiment. A numerical investigation of the nonlinear interactions of low and intermediate frequency modes in [9] has revealed a great wealth of behavior over very narrow regions of parameter space, including a variety of resonances and a number of aperiodic (apparently chaotic) oscillations. A demonstration of this complexity is presented here, the aim being to gain some insight into the ways in which similar experimental oscillations arise, and thereby an understanding of the mechanism of self-excited oscillations in physiological systems.

The following two sections are short summaries of the model and the solutions calculated previously; more detailed discussion may be found in [5, 8, and 10].

2 The Model

The elastic properties of the segment of collapsible tube in Fig. 1 are represented by

$$p - p_e = \mathcal{P}(\alpha) - \frac{1}{2}\alpha_{xx}, \tag{1}$$

where $p(x, t)$ and p_e are the internal and external pressures respectively and $\alpha(x, t)$ is the tube's cross-sectional area (all variables are nondimensional). The terms on the right-hand side of (1) represent separately the effects of transverse and longitudinal stresses in the tube wall. The first term is the "tube law,"

$$\mathcal{P}(\alpha) = \begin{cases} k(\alpha - 1) & \text{if } \alpha \geq 1 \\ 1 - \alpha^{-3/2} & \text{if } \alpha < 1, \end{cases} \tag{2}$$

where $k = 45$ and α is nondimensionalized so that the tube is under zero hoop stress when $\alpha = 1$. When dilated ($\alpha > 1$), the tube is circular in cross-section and has low distensibility; as the tube collapses ($\alpha < 1$) it becomes highly compliant and elliptical; as α falls further the opposite walls of the tube come into contact and the compliance falls. (Because of the discontinuity of $\mathcal{P}'(\alpha)$ at $\alpha = 1$, a slightly smoothed version of (2) with continuous first derivative was used in computations; see [5, 9].) The second term on the right-hand side of (1) represents the contribution to the transmural pressure of constant longitudinal tension in the tube wall; the tube length λ is scaled so that the tension is of unit magnitude.

The mass and momentum conservation equations are

$$\alpha_t + (u\alpha)_x = 0 \tag{3}$$

$$u_t + uu_x = -p_x - d. \tag{4}$$

$u(x, t)$ is the longitudinal velocity, averaged across the cross section of the tube. $d(x, t)$ represents energy dissipation in the flow, which in general has two sources: direct frictional dissipation and energy losses associated with flow separation beyond a constriction in the tube. The former is particularly important when the tube is severely constricted along its length, or completely dilated. In states in which self-excited oscillations are most commonly observed, however (high Reynolds number flows through a tube with a localized constriction), the latter mechanism is more significant [5]. Here, therefore, only the dissipation due to flow separation will be considered. It is represented by

$$d = (\chi - 1)uu_x. \tag{5}$$

$\chi = 1$ (so $d = 0$) upstream of the constriction, where the flow is fully attached and accelerating; $0 < \chi < 1$ ($\chi = 0.2$ arbitrarily) where the flow separates downstream. The point of flow separation $X(t)$ is chosen to be the point at which the flow starts to decelerate, i.e.,

$$u_x(X, t) = 0, \tag{6}$$

so that d increases continuously from zero across X. In steady flow, X coincides with the point of minimum area, and the point at which an adverse pressure gradient develops, although in unsteady conditions these extrema are in general distinct. The position of the true separation point will normally be a short distance downstream of X and will move hysteretically according to the size of the fluctuating adverse pressure gradient [5], so an error is incurred by this quasi-steady approximation (6). This inaccuracy was felt to be acceptable, however, for two reasons. First, there is already some error in the model of dissipation (4). Second, there is considerable numerical advantage in using (6) (as opposed to the criterion used in [5] and [11]), since d is sufficiently smooth across X for computations to be performed using a fixed spatial grid (see Section 3 for details of the numerical method).

The boundary conditions appropriate to an experiment specify that the areas and pressures at each end of the tube match those determined by the rigid parts of the apparatus in Fig. 1:

$$\alpha(0, t) = \alpha(\lambda, t) = 1,$$

$$p(0, t) = p_r - \frac{1}{2}u^2(0, t) - \eta_1 u^2(0, t) - \lambda_1 u_t(0, t),$$

$$p(\lambda, t) = \eta_2 u^2(\lambda, t) + \lambda_2 u_t(\lambda, t). \tag{7}$$

η_i and λ_i represent the resistances and inertances of the upstream ($i = 1$) and downstream ($i = 2$) rigid tubes. Since quantitative comparison between this model and the experiments in [1–3] is not possible [8, 10], the values given to parameters are instead chosen to coincide with those used in [8], so that $\lambda = \eta_1 = \eta_2 = \lambda_1 = \lambda_2 = 1$.

3 Previous Solutions and Numerical Method

The steady solutions of the model were determined in [10], and are parameterized by Q, the flow rate, and $P \equiv p_e - p_2$, the negative of the downstream transmural pressure. For fixed $P > 0$, as Q is increased from zero the tube assumes first a state in which it is collapsed along its length (although held open at each end, see curve (*a*) on Fig. 2); it then begins to widen at its upstream end, and the separation point moves downstream (curve (*b*)); a bulge then develops at the upstream end of the tube, leaving a collapsed neck further downstream (curve (*c*)). Since there is a unique, steady solution over the region of (Q, P)-space of interest here, it is convenient to use Q and P to parameterize *unsteady* solutions also; in computations it is the values of p_r and p_e corresponding to a steady state (given by (7)) which are held constant while the flow rate and internal pressure may vary.

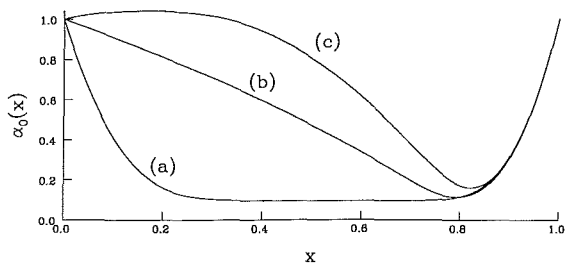

Fig. 2 Three steady states with $P = 30.6$, plotting steady tube area α_0 against x: (*a*) $Q = 0.5$; (*b*) $Q = 1$ and (*c*) $Q = 1.477$. All other parameters are as given in the text.

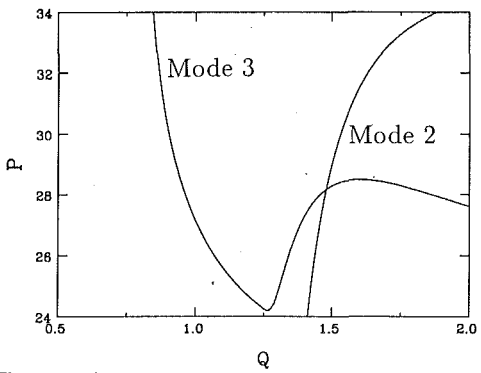

Fig. 3 The neutral curves of modes 2 and 3 are plotted in a region of (Q, P)-space in which they intersect; a steady solution corresponding to (Q, P)-values to the right of the mode 2 neutral curve, or above the mode 3 neutral curve, is linearly unstable to the corresponding mode.

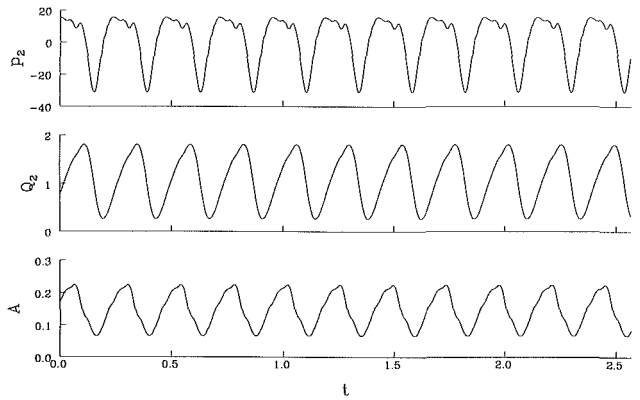

Fig. 4 A time series of the nonlinear mode 3 oscillation with $P = 30.6$, $Q = 1$, showing the downstream pressure $p_2(t)$, downstream flow rate $Q_2(t)$ and minimum area $A(t)$; the corresponding steady state is curve (b) in Fig. 2.

The stability of these steady states to small oscillatory disturbances was determined in [8]. By expressing a small perturbation as a sum of different modes, each mode having its own spatial structure, frequency and growth rate, and linearizing the governing equations in powers of the perturbation amplitude, the regions of (Q, P)-space in which the lower frequency modes become unstable were determined (these regions are bounded by "neutral curves" corresponding to each mode such as shown on Fig. 3). The section of parameter space to be investigated in this paper (within that shown in Fig. 3) was chosen because it is one in which modes "2" and "3" are simultaneously unstable, and is therefore likely to contain interesting dynamical behavior. Mode 2 (3) oscillations in this region have a nondimensional angular frequency of approximately 20 (30), and a half-wavelength very approximately equal to $\lambda/2$ ($\lambda/3$). They were identified in [8] with the low and intermediate frequency oscillations reported in [2].

Hopf bifurcations occur across each of the two neutral curves in Fig. 3. Weakly nonlinear analysis in [8] was used to determine whether these were supercritical or subcritical (in Fig. 3, mode 3 arises subcritically for $1.29 < Q < 1.55$ and supercritically elsewhere; mode 2 is subcritical along the stretch of neutral curve shown). It was also shown in [8] that, since both oscillations arise subcritically at the point of intersection of the two neutral curves, weakly nonlinear interactions between the modes are unstable, and so unobservable, indicating that stable, fully nonlinear interactions must be examined numerically.

MacCormack's method was used to integrate the governing equations of the model. This is an explicit, two-step method which is widely used for problems such as this [5, 11]. A numerical scheme was devised which was shown in [9] to agree with earlier analytical results, correctly reproducing boundaries of stability and regions of sub- and supercriticality, for example. Movement of the separation point X (determined by quartic interpolation using (6)) over the fixed grid could be described satisfactorily provided the dissipation was adequately resolved around X. Between 41 and 101 grid points were sufficient to resolve most tube configurations; the accuracy of the method was established by successive grid refinement. Since the method has a severe stability criterion [5], it was unfortunately not feasible to use finer grids when calculating very long time series. Nonlinear dynamical systems are often extremely sensitive to perturbations of any parameter (such as the number of grid points in a computation), and this will be true of the most dynamically complex oscillation below (Fig. 7); because of the expense of grid refinement this example is presented as a solution of 41 ordinary differential equations approximating Eqs. (1)–(7).

4 Numerical Results

The results presented in this section were calculated assuming that $P = 30.6$, and are chosen to give a flavor of the dynamical behavior of the system rather than a complete picture of the bifurcation structure.

From Fig. 3 it is clear that for small Q a steady, stable state exists resembling curve (a) in Fig. 2. As Q increases through 0.89, a mode 3 oscillation arises through a supercritical Hopf bifurcation. For Q near this bifurcation value the amplitude of the oscillation is small and its waveform sinusoidal; as Q increases the amplitude grows and the waveform becomes increasingly distorted by nonlinearities, as is demonstrated in Fig. 4 which shows the oscillation at $Q = 1$. The downstream pressure $p_2(t)$ varies in a manner characteristic of a relaxation oscillation, having brief periods in which it falls to a low value. The downstream flow rate $Q_2(t)$ varies more smoothly (because of the resistance of the downstream rigid tube η_2) and is slightly delayed in phase (because of the inertance λ_2). The shape of the tube throughout the oscillation is shown in Fig. 5, where $\alpha(x, t)$ is plotted against x and t (the steady tube shape with $Q = 1$ is shown by curve (b) in Fig. 2). The "three-humped" shape of mode 3 oscillations calculated by linear theory in [8] is hard to identify because of the asymmetry of the steady state and the nonlinearity of the oscillation. There is clearly considerable longitudinal movement of the constriction in the tube, and therefore equally vigorous motion of the separation point (recall that this is the point of maximum velocity). During the phase of the oscillation during which p_2 falls below its mean value, the constriction is most severe (as is evident from the time series of the minimum area $A(t)$ in Fig. 4) and it moves very close to the downstream end of the collapsible tube (Fig. 5).

As Q is increased further a secondary Hopf bifurcation occurs and the mode 3 oscillation becomes unstable to a series of quasiperiodic states. These have two fundamental frequencies, one the original mode 3 frequency (ω_3) and the other, ω_2, arising from the growing influence of mode 2 (note from Fig. 3 that for $P = 30.6$ the steady state becomes subcritically unstable to mode 2 oscillations when $Q = 1.56$). A time series of a such an oscillation is presented in Fig. 6, for which $Q = 1.45$ (note the very different time scale to that used in Fig. 4). Over much of this region of parameter space ω_2 and ω_3 are "locked" in rational ratios, i.e., $\omega_2/\omega_3 = p/q$ for some integers p and q, so that the resulting oscillation repeats itself exactly after a finite time. In the case of Fig. 6 this was confirmed by construction of a return map, which showed that the oscillation has a period of exactly $27T_3$ (≈ 6 time units), where $T_3 = 2\pi/\omega_3$ is the period of the mode 3 component. In addition, for the majority of this $27T_3$-cycle the time series comes close to

repeating itself after times of $3T_3$. Further calculations in [9] have shown that the system is close to a region of parameter space in which there is a "strong" resonance with $\omega_2/\omega_3 = 2/3$, in which oscillations have a period of exactly $3T_3$. These resemble Fig. 6 except that they lack the slow modulation of period $27T_3$, and are characterized by every third constriction of the tube being more severe than the others.

For larger Q the system passes rapidly through a number of different states; one example of these is presented in Fig. 7, showing a long section of a p_2-time series of the oscillation at $Q = 1.477$. This is only part of a much longer computation; from that there was no evidence that this behavior was either repetitive or transient. Although distinct patterns in the time series are evident, some resembling the quasiperiodic behavior in Fig. 6 (e.g., $23 < t < 43$), others having severe modulation at a low frequency apparently unrelated to ω_2 or ω_3 ("bursting," $55 < t < 85$), no long-term recurrent structure could be identified. The system often passes through very similar states at different times in its cycle (e.g., $t = 26$ and $t = 89$), but comparison of the time series beyond each point always shows that the two paths followed by the oscillation diverge: the system appears to show sensitivity to initial conditions, an indication that this oscillation may be chaotic. Construction of phase portraits and return maps [9] only serve to demonstrate an extremely complicated topological structure.

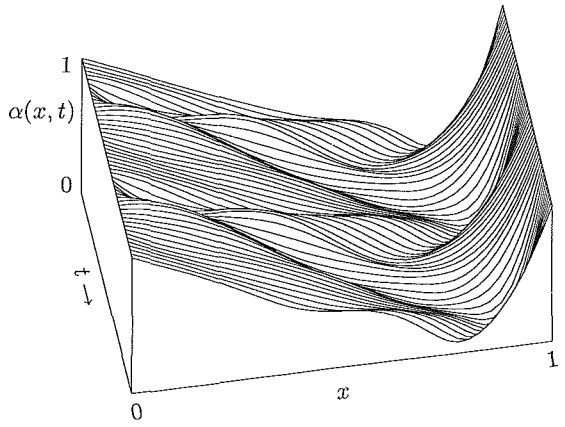

Fig. 5 The varying tube area $\alpha(x, t)$ during the course of the oscillation shown in Fig. 4 is plotted as a function of space and time.

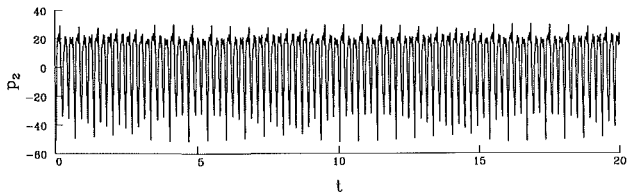

Fig. 6 A time series of a nonlinear quasiperiodic oscillation at $Q = 1.45$, $P = 30.6$; this is a mode-locked state, with the frequencies of the underlying mode 2 and mode 3 oscillations rationally related.

Unfortunately once the amplitude of the oscillations becomes too great, (e.g., once Q exceeds about 1.5 with $P = 30.6$), the solutions of this model develop an unexpected inconsistency. Multiple extrema arise in the distribution of velocity in the tube, so that to ensure continuity of d (Eq. (5)) it becomes necessary to split the single region of dissipation at the tube's downstream end into two, which results in a region of attached, accelerating flow between two regions of separated, decelerating flow. This feature is not believed to be physically realistic since it does not take account of the downstream advection of dissipative eddies generated in the upstream region of separation. In the examples above (e.g., Figs. 6 and 7) these additional regions of dissipation are weak and short-lived, and are not believed to give rise to significant errors. Elsewhere, however, this becomes a significant problem, and restricts the range of parameter space that can be explored.

5 Discussion

Despite the success of this model in describing steady flows, multiple modes of oscillation and complex nonlinear behavior, the difficulties described above that arise for very vigorous oscillations suggest an inadequacy in this model's representation of flow separation (5, 6). The quasi-steadiness inherent in (6) is one potential shortcoming, but any future improvements in this model, such as allowing hysteresis in the motion of the separation point (which is likely to add further richness to an already complex system), should go hand-in-hand with improvements in the description of energy loss.

Nevertheless this model does describe a number of experimental observations. The relaxation waveform of the mode 3 time series in Fig. 4 resembles the repetitive, intermediate frequency oscillations described in [1] and [3] (the p_2-waveform of an experimental I oscillation is shown in Fig. 8(*a*)), although the proportion of the period during which p_2 falls below its mean level is longer than observed experimentally and there are minor differences between the waveforms. (It must be remembered that because thick-walled tubes were used in [1] and [3], while the model requires the wall to be thin, it was

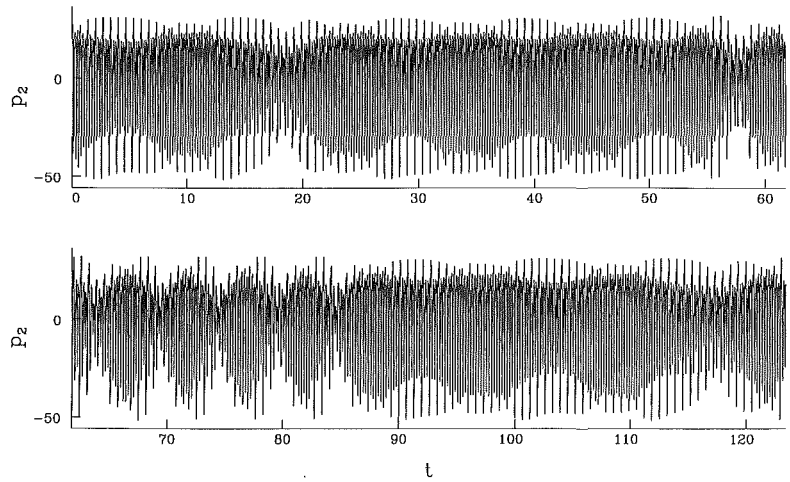

Fig. 7 A continuous time series of an aperiodic oscillation at $Q = 1.477$, $P = 30.6$; the corresponding steady state is curve (*c*) in Fig. 2.

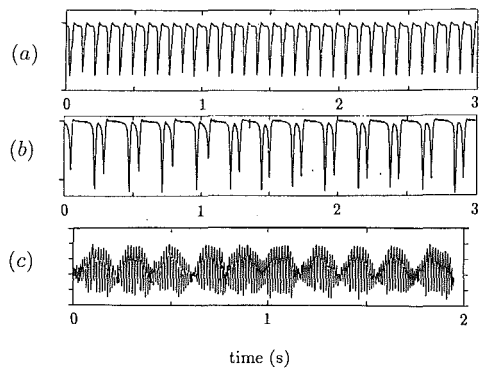

Fig. 8 Three experimental oscillations (reproduced from [3], with permission), showing p_2 as a function of time. (*a*) An intermediate-frequency (I) oscillation of 11.1 Hz. (*b*) A "multiple collapse" oscillation at 4.06 Hz. The period corresponds to that of an L oscillation, the time between the closest spikes matches the period of an I oscillation. (*c*) A slowly modulated H oscillation, frequency 70 Hz.

not possible to match parameters.) It would be valuable to establish the accuracy of the predicted shape of the tube in Fig. 5 (to the author's knowledge no such measurements are yet published), as this would aid interpretation of the shape of the waveforms. Features such as the small fluctuations in the p_2-waveform in Fig. 4 at the top of its cycle, for example, are of interest in this respect. It is likely that these fluctuations arise from the brief phase of the oscillation during which the constriction becomes most severe and moves furthest downstream (Fig. 5). The sudden and very substantial deceleration of the flow beyond the constriction during this phase leads to a rapid increase in the amount of dissipation d (see (5)); abrupt variations in d generate pressure disturbances that propagate dispersively up and down the tube, reflect from the junctions with the rigid segments at either end, and give rise to these fluctuations.

The numerical results suggest that much of the complex dynamical behavior observed experimentally arises through the nonlinear interaction of distinct modes of oscillation. Mode locking (e.g., Fig. 6) is a widespread phenomenon, and is likely to be responsible for the "multiple collapse" oscillations described in [1, 2, 3]. Figure 8(*b*) shows an example of such an oscillation from [3], which appears to arise from interacting L and I components with frequencies in the ratio 1 to 3. Such a ratio (and the corresponding waveform) was never observed in the present study, but a strong resonance bearing a clear similarity to this example, with $\omega_2/\omega_3 = 2/3$ (with one strong and two weaker minima in the p_2-waveform, described in Section 4), was a robust phenomenon. "Bursting," which occurs transiently in Fig. 7 ($55 < t < 85$) and which for a range of parameter values can also be sustained indefinitely [9], has a strong resemblance to an oscillation recorded in [3] and shown in Fig. 8(*c*) (albeit a modulated H, rather than I, oscillation). These computations indicate also that it may be an indication of aperiodic or chaotic behavior in nearby regions of parameter space.

Acknowledgment

This work was carried out under the support of a Science and Engineering Council Research Studentship and a bursary from Smith Associates Ltd. The author would like to express his gratitude to Prof. T. J. Pedley for his excellent guidance and advice.

References

1 Bertram, C. D., "Unstable Equilibrium Behavior in Collapsible Tubes," *J. Biomech.*, Vol. 19, 1986, pp. 61–69.

2 Bertram, C. D., Raymond, C. J., and Pedley, T. J., "Mapping of Instabilities for Flow Through Collapsed Tubes of Differing Length," *J. Fluids Structures*, Vol. 4, 1990, pp. 125–153.

3 Bertram, C. D., Raymond, C. J., and Pedley, T. J., "Application of Nonlinear Dynamics Concepts to the Analysis of Self-Excited Oscillations of a Collapsible Tube Conveying a Fluid," *J. Fluids Structures*, Vol. 5, 1991, pp. 391–426

4 Bonis, M., and Ribreau, C., "Etude de Quelques Propriétés de l'Écoulement dans une Conduite Collabable," *La Houille Blanche*, Vol. 3/4, 1978, pp. 165–173.

5 Cancelli, C., and Pedley, T. J., "A Separated-Flow Model for Collapsible-Tube Oscillations," *J. Fluid Mech.*, Vol. 157, 1985, pp. 375–404.

6 Conrad, W. A., "Pressure-Flow Relationships in Collapsible Tubes," *IEEE Trans. Bio-med. Engng*, Vol. BME-16, 1969, pp. 284–295.

7 Danaky, D. T., and Ronan, J. A., "Cervical Venous Hums in Patients on Chronic Hemodialysis," *New Eng. Jour. Med.*, Vol. 291, 1974, pp. 237–239.

8 Jensen, O. E., "Instabilities of Flow in a Collapsed Tube," *J. Fluid Mech.*, Vol. 220, 1990, pp. 623–659.

9 Jensen, O. E., "Flow in Collapsible Tubes," Ph.D. thesis, 1990, University of Cambridge.

10 Jensen, O. E., and Pedley, T. J., "The Existence of Steady Flow in a Collapsed Tube," *J. Fluid Mech*, Vol. 206, 1989, pp. 339–374.

11 Matsuzaki, Y., and Matsumoto, T., "Flow in a Two-Dimensional Collapsible Channel with Rigid Inlet and Outlet," ASME JOURNAL OF BIOMECHANICAL ENGINEERING, Vol. 111, 1989, pp. 180–184.

12 Shapiro, A. H., "Physiologic and Medical Aspects of Flow in Collapsible Tubes," *Proc. 6th Canadian Congr. Appl. Mech.*, 1977, pp. 883–906.

13 Ur, A., and Gordon, M., "Origin of Korotkoff Sounds," *Am. J. Physiol.*, Vol. 218, 1970, pp. 524–529.